Journal of research and development

| | 233 | Preface |
|--|-----|--|
| R. A. Myers and J. C. Tamulis | 234 | Introduction to Topical Issue on Non-Impact Printing Technologies |
| M. H. Lee, J. E. Ayala, B. D. Grant, W. Imaino, A. Jaffe, M. R. Latta, and S. L. Rice | 241 | Technology Trends in Electrophotography |
| R. C. Miller, Jr. | 252 | Introduction to the IBM 3800 Printing Subsystem Models 3 and 8 |
| David McMurtry, Mike Tinghitella, and Roger Svendsen | 257 | Technology of the IBM 3800 Printing Subsystem Model 3 |
| C. Barrera and A. V. Strietzel | 263 | Electrophotographic Printer Control as Embodied in the IBM 3800 Printing Subsystem Models 3 and 8 |
| J. L. Crawford, C. D. Elzinga, and R. Yudico | 276 | Print Quality Measurements for High-Speed Electrophotographic Printers |
| J. Borch and R. G. Svendsen | 285 | Paper Material Considerations for System Printers |
| Gerald W. Baumann | 292 | Flash Fusing in Electrophotographic Machines |
| Richard H. Darling, Chen-Hsiung Lee, and Lawrence Kuhn | 300 | Multiple-Nozzle Ink Jet Printing Experiment |
| F. C. Lee, R. N. Mills, and F. E. Talke | 307 | The Application of Drop-on-Demand Ink Jet Technology to Color Printing |
| D. B. Bogy and F. E. Talke | 314 | Experimental and Theoretical Study of Wave Propagation Phenomena in Drop-on-Demand Ink Jet Devices |

| J. E. Fromm | 322 | Numerical Calculation of the Fluid Dynamics of Drop-on-Demand Jets |
|-------------|-----|---|
| | 334 | Recent papers by IBM authors |
| | 337 | Patents |

Flash Fusing in Electrophotographic Machines

A theoretical model of the flash fusing process for electrophotographic machines was developed using the joint solution of a nonlinear circuit equation and the one-dimensional thermal diffusion equation. Numerous experiments were run using different toners according to the size of toner particles and the pulse width in order to determine the minimum energy that was required for fusing. The experiments confirm that this model predicts reasonably well what was observed in the lab. The melt depth required for good fusing is slightly less than mean particle size. At that depth the temperature is somewhat greater than the temperature required in the nip of a hot roll fuser for the same toner. Under typical flash fusing, the top surface of the toner is subjected to considerably higher temperatures than the melt temperature of the toner. From the combined analytical and experimental results, the proper compromises can be made for efficiency and volatiles.

Introduction

Flash fusing technology for electrophotographic machines has been under development for more than 25 years. IBM's first patent in this art was obtained in 1957 [1]. Today Agfa-Gevaert and Fujitsu manufacture flash fusing machines with throughputs from 15 to 215 pages per minute.

The purpose of the present study was to develop and confirm a theoretical model of the flash fusing process. Using this model, a design engineer can study trade-offs and compromises needed to optimize real systems. The process includes storing energy in a capacitor and then discharging it through a flash tube. The radiated energy is absorbed in the toner pigment and converted into heat. The heat diffuses through the toner, causing it to melt and flow onto the paper. The toner then cools and hardens, "fixing" itself to the document.

This paper contains five main sections. The first presents the electro-optical analysis of the flash tube in the pulse-forming network. The second couples the network to the surface temperature of the toner. The third couples the toner/paper interface temperature to the pulse-forming network. In the fourth, these results are used to analyze systems and understand design trade-offs. Finally, the fifth section presents the experimental confirmation of the model.

Analysis of the flash tube and drive circuit

Figure 1 shows the circuit typically used to drive a flash tube. The capacitor C_0 stores the energy, which is converted to optical radiant output in the arc. R is the dc resistance of the entire circuit except for the tube. The circuit resistance is primarily the resistance of the inductor and capacitor. The inductor L is added to the circuit to tailor the pulse and eliminate the initial surge current.

Current reversals destroy flash tubes very early in life. For this reason the inductance is not allowed to be so large as to cause "ringing." Hence, the current is always assumed positive. The voltage across the tube is related to the current by [2]

$$V = K_0 i^{1/2}, (1)$$

where

$$K_0 \simeq 1.275 \left(\frac{tube \ arc \ length}{tube \ bore} \right) \times \left(\frac{fill \ pressure}{60 \ 000 \ Pa} \right)^{0.2} \text{ volt-amp}^{-1/2}.$$
 (2)

The circuit equation then becomes [3]

$$L\frac{di}{dt} + Ri + \frac{1}{C_0} \int_0^t id\hat{t} + K_0 i^{1/2} = V_0,$$
 (3)

Copyright 1984 by International Business Machines Corporation. Copying in printed form for private use is permitted without payment of royalty provided that (1) each reproduction is done without alteration and (2) the *Journal* reference and IBM copyright notice are included on the first page. The title and abstract, but no other portions, of this paper may be copied or distributed royalty free without further permission by computer-based and other information-service systems. Permission to *republish* any other portion of this paper must be obtained from the Editor.

where V_0 is the capacitor voltage before ignition.

The appropriate nondimensionalizing of time is achieved by

$$T = t \frac{V_0}{K_0^2 C_0} \,.$$
(4)

The appropriate nondimensionalizing of current is found in

$$I = i \left(\frac{K_0}{V_0}\right)^2. \tag{5}$$

The inductance is nondimensionalized by

$$\Phi = \frac{L}{C_0} \left(\frac{V_0}{K_0^2} \right)^2, \tag{6}$$

and the circuit resistance is nondimensionalized by

$$\Psi = \frac{RV_0}{K_0^2} \,. \tag{7}$$

The circuit is written in fully dimensionless form as

$$\Phi \frac{dI}{dT} + \Psi I + \int_0^T I d\hat{T} + I^{1/2} = 1.$$
 (8)

The solutions to the circuit equations can be tabulated for all cases as a two-parameter family of solutions involving the dimensionless inductance Φ and the dimensionless circuit resistance Ψ . Figure 2 shows the current profiles for various values of Φ , with $\Psi=0$. Figure 3 shows the instantaneous power.

The total energy dissipated in the flash tube prior to time t is

$$\int_0^t K_0 i^{3/2} d\hat{t}.$$

If this is normalized with respect to the initial capacitor energy, the dimensionless energy then becomes

$$2\int_0^T I^{3/2}d\hat{T}.$$

Figure 4 shows these plots. Figure 5 shows how the power pulse width varies with inductance when the circuit has no resistance.

Figures 2 through 5 include values of dimensionless inductance Φ from 0 to 2.5. The onset of ringing occurs for $2 < \Phi < 2.5$. At $\Phi = 2.5$, the ringing is negligible, and may actually not occur if the reverse bias on the capacitor is insufficient to restrike the arc. Values of Φ greater than 2.5 should be avoided to prevent flash tube damage; hence, they were not studied.

Figures 6, 7, and 8 show the current, power, and energy profiles with resistance in the drive circuit. They compare

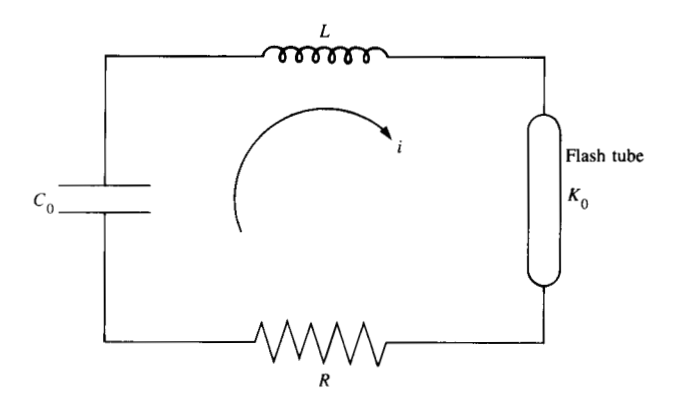


Figure 1 Flash tube drive circuit.

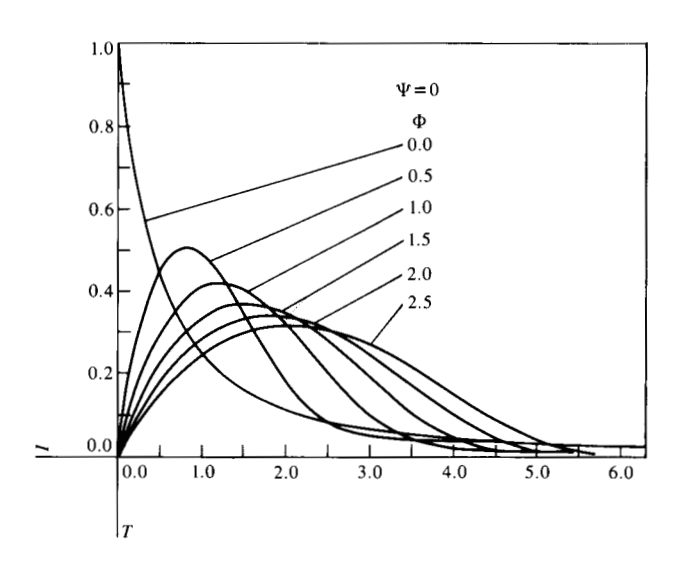


Figure 2 Current in flash tube vs time, with no circuit resistance.

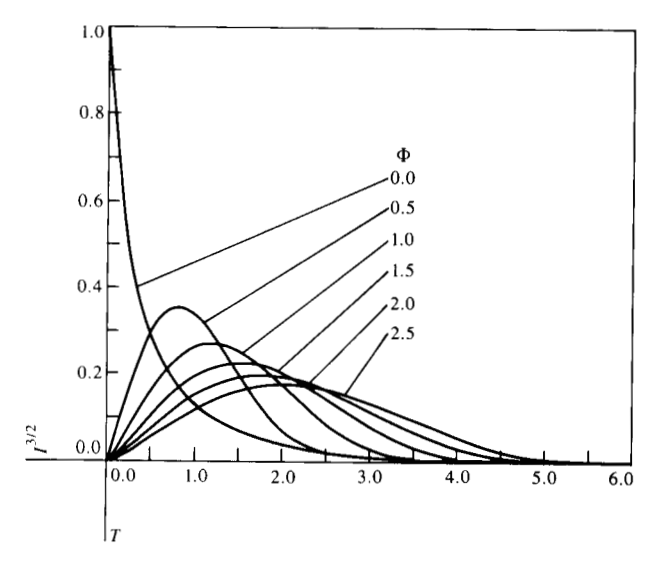


Figure 3 Power dissipated in flash tube vs time, with no circuit resistance.

293

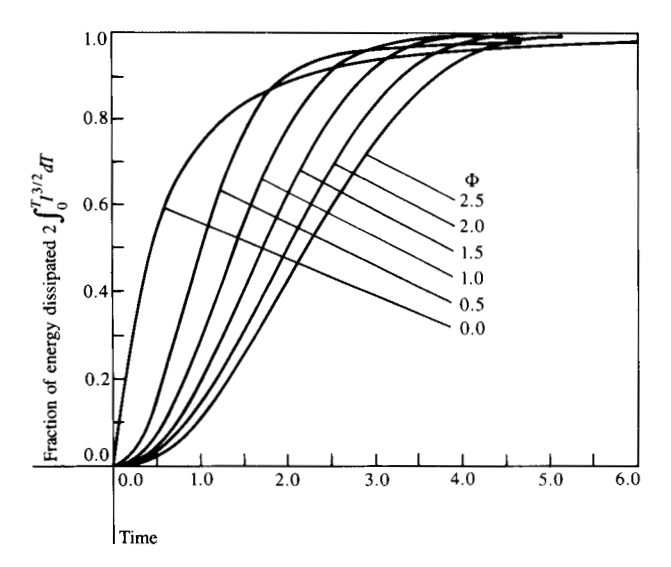


Figure 4 Energy dissipated in flash tube vs time, with no circuit resistance.

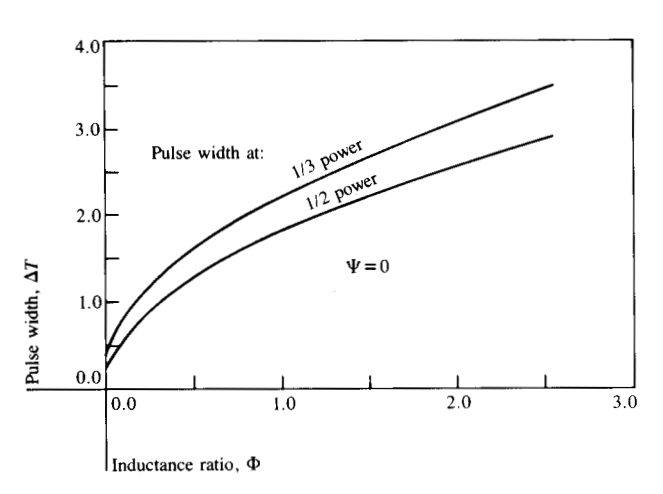


Figure 5 Power pulse width in flash tube vs inductance, with no circuit resistance.

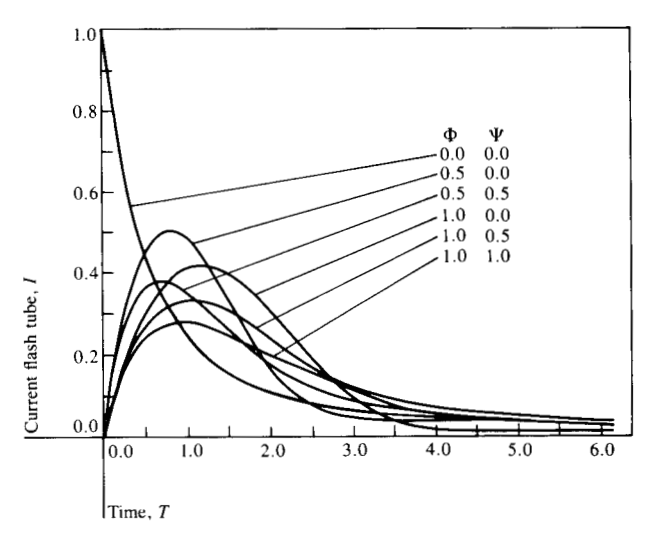


Figure 6 Current in flash tube vs time.

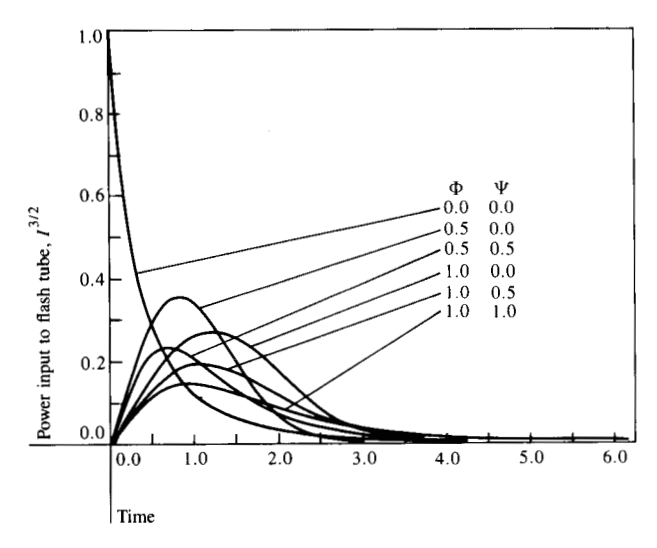


Figure 7 Power dissipated in flash tube vs time.

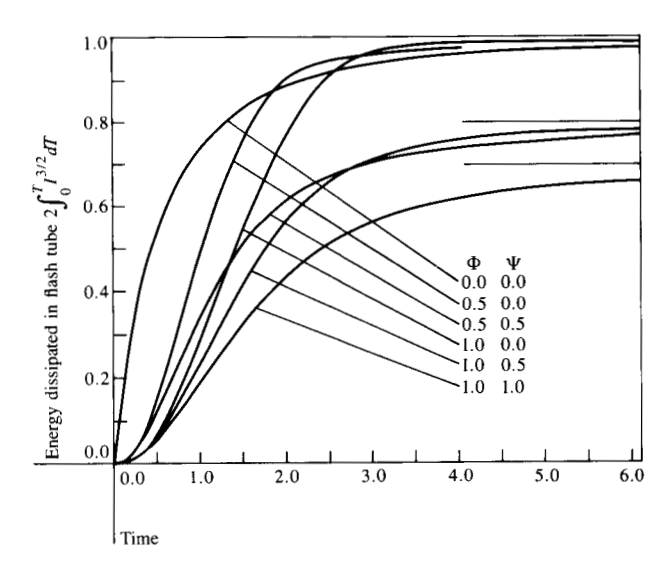


Figure 8 Energy dissipated in flash tube vs time.

directly to Figs. 2, 3, and 4. The effects of circuit resistance are readily seen. The solutions shown thus far are all numerical approximations; exact solutions exist only for $\Phi = 0$.

Circuit losses were tabulated numerically and found to be independent of inductance to within the numerical accuracies of the solution. This is unusual for a nonlinear circuit. The range of values tested was $0 < \Phi < 2.5$ and $0 < \Psi < 1$. In a typical circuit, Ψ may be less than 0.1 and should rarely exceed 0.5. To estimate the circuit efficiency, the closed-form solution was obtained from the circuit equation with no choke coil:

$$\Psi I + I^{1/2} = 1 - \int_0^T I d\hat{T}. \tag{9}$$

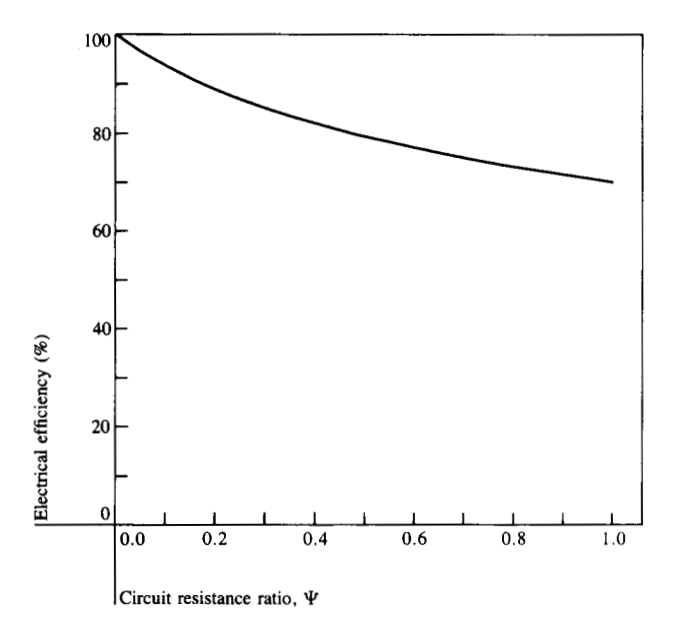


Figure 9 Circuit efficiency vs circuit resistance.

The wasted energy, $E_{\rm R}$, is computed from

$$E_{\rm R} = \int_0^\infty R i^2 d\hat{t}. \tag{10}$$

Rewritten in dimensionless form, (10) becomes

$$\frac{E_{\rm R}}{\frac{C_0 V_0^2}{2}} = 2\Psi \int_0^\infty I^2 d\hat{T}.$$
 (11)

Obtaining the solution to (9) and integrating (11) results in

$$\frac{E_{\rm R}}{\frac{C_0 V_0^2}{2}} = \frac{\left(\sqrt{1 + 4\Psi} - 1\right)^3}{16\Psi^2} \left(\sqrt{1 + 4\Psi} + 1/3\right). \tag{12}$$

Equation 12 shows the fraction of energy wasted in the drive circuit. Subtracting this value from 1.0 gives the circuit efficiency shown in **Figure 9**.

In most flash fuser drive circuits the resistance can be kept small enough to ignore. When the resistance is small, a good approximation to the circuit solutions is

$$I^{3/2} \simeq \beta^2 T e^{-\beta^2 T^2},\tag{13}$$

where

$$\beta = 0.623\Phi^{-0.445}.\tag{14}$$

The agreement is excellent for $0.25 < \Phi < 2.5$. An apparent small time shift arises, which has no effect on the subsequent heat transfer study. **Figures 10** and **11** show the power and energy profiles from this approximation. The approximation

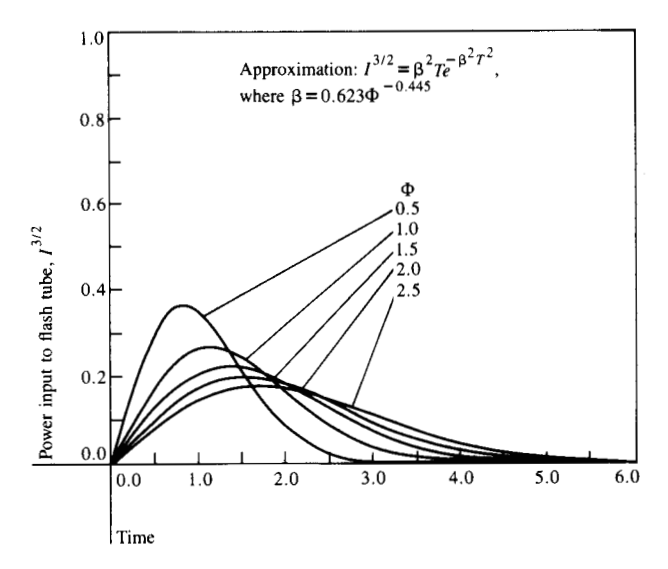


Figure 10 Approximate power dissipation in flash tube vs time.

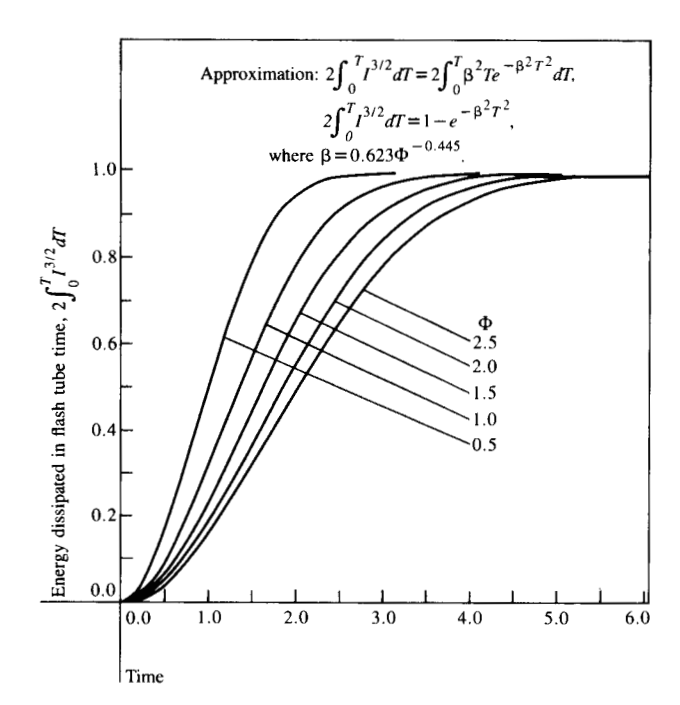


Figure 11 Approximate energy dissipated in flash tube vs time.

greatly simplifies the circuit design and eliminates the need for more numerical solutions to Eq. (8).

Analysis of the surface temperatures

The toner surface being heated is modeled by the one-dimensional diffusion equation in a semi-infinite half space initially at thermal equilibrium. The half-space has volumetric heat capacity c with units Jm^{-3} (°C)⁻¹ and thermal conductivity k

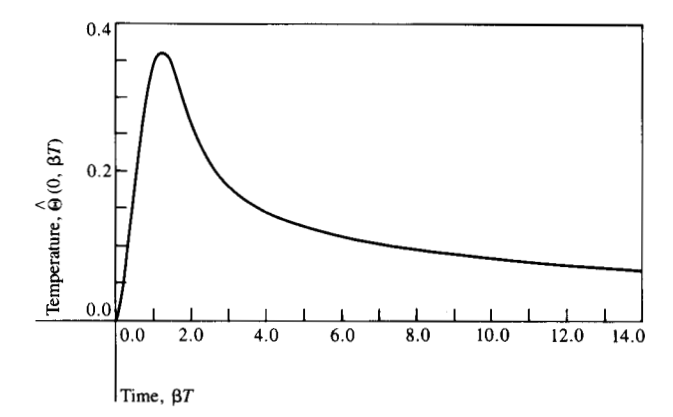


Figure 12 Surface temperature vs time.

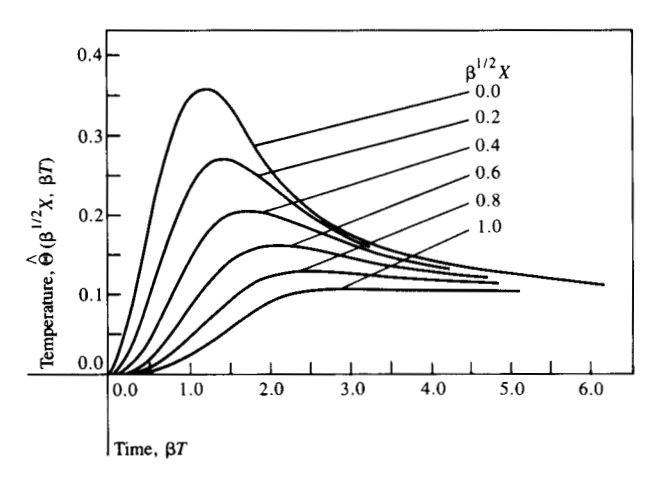


Figure 13 Surface and subsurface temperature profiles for inductance-limited xenon flash.

with units $Jm^{-1}-s^{-1}$ (°C)⁻¹. The half-space is governed [4] by the equation

$$c\frac{\partial\Theta}{\partial t} = k\frac{\partial^2\Theta}{\partial x^2},\tag{15}$$

where Θ is the relative temperature in the toner in °C and x is the depth into the toner in m.

The temperature of the top surface is then [4, 5]:

$$\Theta(0, i) = \frac{1}{\sqrt{\pi c k}} \int_0^t \frac{q(\tau)}{\sqrt{t - \tau}} d\tau, \tag{16}$$

where q is the power input per unit area in $Jm^{-2}-s^{-1}$.

Using the Faltung Theorem [6], the singularity in the integrand is moved from the end of the interval to the beginning:

$$\Theta(0, t) = \frac{1}{\sqrt{\pi c k}} \int_0^t \frac{q(t - \tau)}{\sqrt{\tau}} d\tau.$$
 (17)

Then time is nondimensionalized by

$$T = \frac{t}{t_0},\tag{18}$$

and the singularity is removed from the integrand by the transformation

$$\zeta = \sqrt{\tau/t_0} \,. \tag{19}$$

Using (18) and (19) in (17) gives

$$\Theta(0, T) = \frac{2\sqrt{t_0}}{\sqrt{\pi ck}} \int_0^{\sqrt{T}} q(T - \zeta^2) d\zeta.$$
 (20)

The input power q is found from the circuit equation and Eq. (1):

$$q = \xi K_0 i^{3/2}, (21)$$

where ξ has the units m⁻².

The parameter ξ is simply the efficiency of the flash tube circuit and reflector divided by the area covered by the reflector. Coupling Eqs. (5), (20), and (21) gives

$$\Theta(0, T) = \frac{2\sqrt{t_0}\xi V_0^3}{\sqrt{\pi c k} K_0^2} \int_0^{\sqrt{T}} \{I(T - \zeta^2)\}^{3/2} d\zeta.$$
 (22)

Applying the approximation for power in Eq. (13) to Eq. (22) gives

$$\Theta(0, T) = \frac{2\sqrt{t_0}\xi V_0^3 \beta^2}{\sqrt{\pi c k} K_0^2} \int_0^{\sqrt{T}} (T - \zeta^2) e^{-\beta^2 (T - \zeta^2)^2} d\zeta.$$
 (23)

The temperature is nondimensionalized as follows:

$$\hat{\Theta}(0, T) = \Theta(0, T) \left\{ \frac{\sqrt{\pi c k} K_0}{2\sqrt{C_c \varepsilon} V_0^{5/2} \sqrt{\beta}} \right\}.$$
 (24)

Two new dummy variables are defined:

$$\hat{T} = \beta T, \tag{25}$$

$$\hat{\zeta} = \sqrt{\beta}\zeta. \tag{26}$$

These new variables are combined in (24), resulting in

$$\hat{\Theta}(0,\,\hat{T}) = \int_0^{\sqrt{T}} (\hat{T} - \hat{\zeta}^2) e^{-(T - \hat{\zeta}^2)^2} d\hat{\zeta}. \tag{27}$$

Equation (27) gives the dimensionless surface temperature as a function of circuit, tube, reflector, and toner design. It has no singularities and it was tabulated numerically. Figure 12 shows a plot of surface temperature vs time.

Analysis of the paper-toner interface temperatures

The temperatures beneath the surface of the toner are obtained from the solution of the diffusion equation in a semi-infinite half-space. If a half-space is initially at thermal equilibrium and a step change in temperature $\Delta\Theta$ occurs at the surface at time zero, the resulting temperature in the body [4] is

$$\Theta(x, t) = \Delta \Theta \operatorname{erfc} \left\{ \sqrt{\frac{c}{4k}} \frac{x}{\sqrt{t}} \right\},$$
(28)

where erfc is the complementary error function.

For an arbitrary surface temperature [4],

$$\Theta(x, t) = \int_0^t \frac{d\Theta(0, \tau)}{d\tau} \operatorname{erfc} \left\{ \sqrt{\frac{c}{4k}} \frac{x}{\sqrt{t - \tau}} \right\} d\tau.$$
 (29)

By using integration by parts and applying the Faltung Theorem, Eq. (29) can be transformed to

$$\Theta(x, t) = \frac{1}{\sqrt{\pi}} \int_0^t \Theta(0, t - \tau)$$

$$\times \left\{ e^{-\frac{c x^2}{4k\tau}} \sqrt{\frac{c}{4k}} \frac{x}{\tau^{3/2}} \right\} d\tau. \quad (30)$$

A new, dimensionless depth into the toner surface is defined by

$$X = \sqrt{\frac{c}{4k}} \frac{x}{\sqrt{t_0}},\tag{31}$$

where

$$t_0 = \frac{K_0^2 C_0}{V_0} \,. \tag{32}$$

Equation (32) is consistent with all prior development. Combining (4), (18), (19), (30), and (31) gives the result

$$\Theta(x, T) = \frac{2x}{\sqrt{\pi}} \int_{\frac{1}{\sqrt{x}}}^{\infty} \Theta\left(0, T - \frac{1}{\zeta^2}\right) e^{-x^2 \xi^2} d\zeta.$$
 (33)

Noting that Eq. (33) is linear in temperature, and recognizing that the relevant depth parameter consistent with the normalized circuit solution is $\beta^{1/2}X$, Eq. (33) can be put in the alternate form

$$\hat{\Theta}(\beta^{1/2}X, \beta T)$$

$$=\frac{2\beta^{1/2}X}{\sqrt{\pi}}\int_{(\beta T)^{-1/2}}^{\infty}\hat{\Theta}\left(0,\,\beta T-\frac{1}{\zeta^2}\right)e^{-(\beta^{1/2}X)^2\zeta^2}d\zeta.$$
 (34)

The function $\Theta(0, \beta T)$ was computed in the previous section. Figure 13 shows the integral computed in (34).

Evaluating systems and their trade-offs

A flash fuser has three primary functional objectives. First, the fuser must fuse toner to paper. Second, it should use as little energy as possible to do this. Third, the surface overtemperature must be kept down to a reasonable level to limit generation of volatiles.

The overtemperature shown in Figure 13 can be plotted as a function of heating depth, as in Figure 14. Or it can be

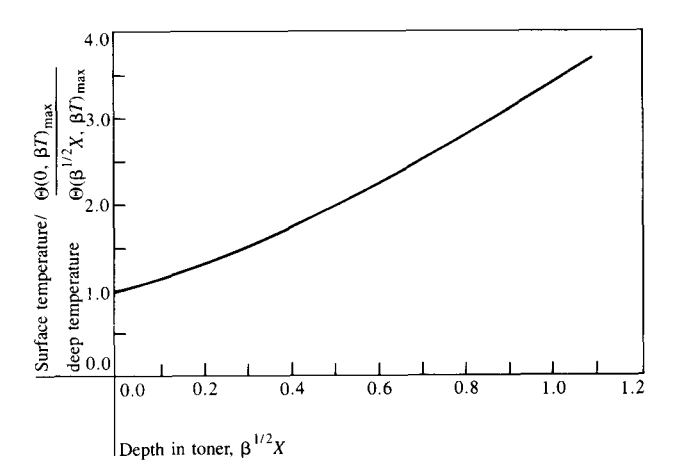


Figure 14 Surface overtemperature vs depth in toner for inductancelimited xenon flash.

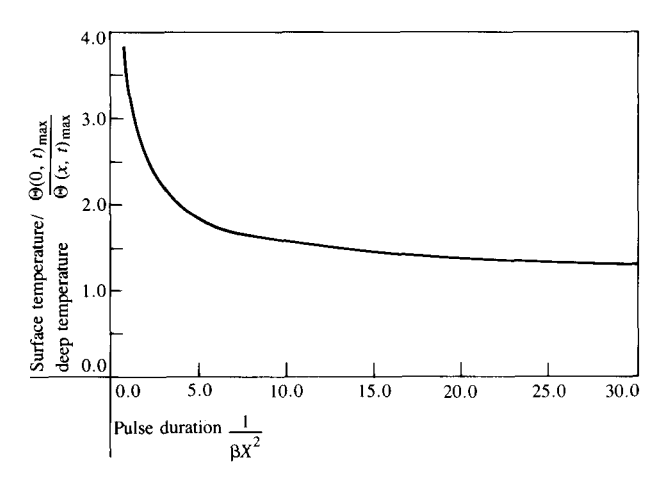


Figure 15 Surface overtemperature vs xenon flash pulse duration.

plotted as a function of flash pulse duration, as in **Figure 15**. How short flashes can greatly overheat the toner surface is readily apparent.

The energy or thermal efficiency can also be defined as

$$\frac{xc[\Theta(x,t)]_{\text{max}}}{\frac{\xi C_0 V_0^2}{2}}$$

where x is the thickness of the toner layer.

Figure 16 shows the efficiency

$$\frac{xc[\Theta(x,t)]_{\text{max}}}{\frac{\xi C_0 V_0^2}{2}} = \frac{8}{\sqrt{\pi}} (\beta^{1/2} X) \hat{\Theta}(\beta^{1/2} X, \beta T)_{\text{max}}.$$
 (35)

Plotting inverse efficiency, **Figure 17** shows the relationship between required energy and flash duration.

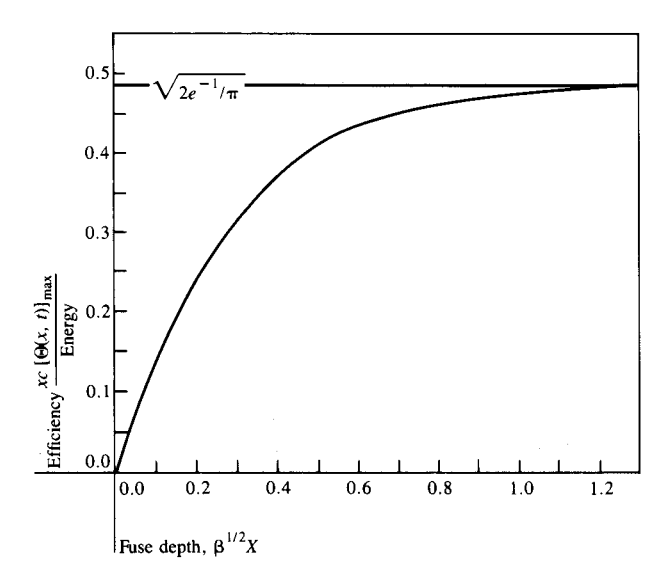


Figure 16 Thermal efficiency vs heating depth.

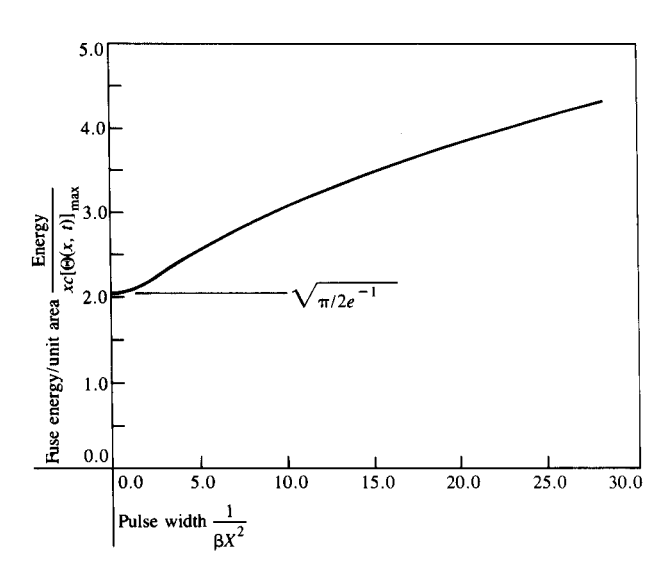


Figure 17 Energy required to reach subsurface temperatures vs xenon flash pulse duration.

Notice that the long pulse durations that produce minimal overtemperatures also require larger energies. Short flash durations require minimum energy but produce maximum overtemperatures. Hence, a compromise must be sought.

In a system design, the engineer must determine the depth of toner to be fused, the temperature required to achieve melt and flow, and the overtemperature that can be tolerated. From Figure 15, the pulse width can be determined for a particular overtemperature

$$\frac{1}{\beta X^2} = \frac{2.865 k \Delta t}{c x^2},$$

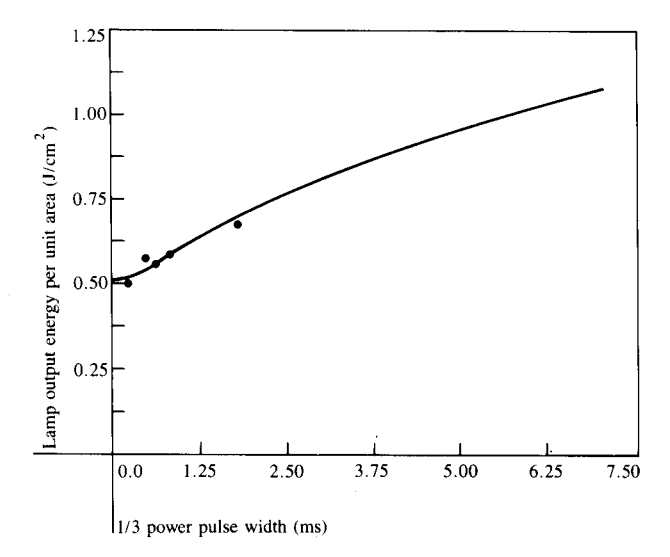


Figure 18 Comparison of energy required to fuse vs pulse duration—theory vs experiment.

where Δt is the 1/3 power pulse width for the flash tube and x is the fuse depth. Note that $\beta T = 1.396$ when T is the 1/3 power pulse width. The energy output from the flash can then be computed from Fig. 17, using the same value for $1/\beta X^2$.

Experimental results

The fundamental relationships between the flash tube and pulse-forming network have been well understood and confirmed daily in literally millions of optical systems over the past twenty years. No additional experiments are presented in this paper.

A number of experiments were run with a variety of toners, jet milled to a variety of particle sizes. Volatiles were found to increase as a strong function of toner surface temperature. The absolute levels and constituents of the volatiles depend on the chemistry of the toner (i.e., epoxy, vinyl, etc.) and the volatile-suppressing additives. In a general way, these data confirmed the surface temperature model.

More important, the minimum energy required to fuse was related to toner particle size and pulse width. **Figure 18** shows a typical set of data. The toner was IBM 825, jet milled to a mean particle size of 13.5×10^{-6} m. This toner fuses in an IBM Series III copier with a hot roll fuser. In the hot roll nip, the toner is expected to reach approximately 110° C. At this temperature, it softens considerably but still requires high pressures to fuse. The solid line in Figure 18 is a theoretical plot of energy vs pulse width for a toner with heat capacity and thermal conductivity matched to 825 toner. The fuse depth was 9.4×10^{-6} m and the melt temperature was 180° C. The experimental results were about as expected: the toned image includes a large fraction of "fines" less than 13.5×10^{-6}

m, which fill in between and below the larger particles. Hence, the typical fuse depth is expected to be slightly less than the mean particle size. The absence of pressure in the flash fuser requires temperatures above the 110°C nip in the hot roll; 180°C is in the expected range of temperature.

Numerous experiments were run on different toners. The results confirm that the model predicts reasonably well what is observed in the lab.

Conclusions

The flash fusing process can be modeled by the joint solution of a nonlinear circuit equation and the one-dimensional thermal diffusion equation. Experimental results observed in the laboratory confirm this joint solution. By combining the analytical model with laboratory experiments, the proper compromises can be made to maximize efficiency while minimizing generation of volatiles.

From the combined analytical and experimental results, the melt depth required for good fusing is slightly less than the mean particle size. The temperature at that depth is somewhat greater than the temperature required in the nip of a hot roll fuser for the same toner. Under typical flash fusing, the top surface of the toner is subjected to considerably higher temperatures than the melt temperature of toner.

Acknowledgments

The author expresses his appreciation to Carl Hutchings of the IBM Boulder Laboratory for the experimental data presented in this paper. The author also expresses his appreciation to P. Bruce Newell of GTE Sylvania for his insights into flash tube characteristics.

References

- D. D. Roshon, Jr., "Xerographic Image Fixing Apparatus," U.S Patent 2,807,703, September 24, 1957.
- J. H. Goncz, "Resistivity of Xenon Plasma," J. Appl. Phys. 36, No. 3, 742-743 (1965).
- J. P. Markiewicz and J. L. Emmett, "Design of Flashlamp Driving Circuits," *IEEE J. Quantum Electron.* QE-2, No. 11, 707-711 (1966).
- H. S. Carslaw and J. C. Jaeger, Conduction of Heat in Solids, Clarendon Press, Oxford, England, 1965.
- R. V. Churchill, Operational Mathematics, McGraw-Hill Book Co., Inc., New York, 1958.
- C. R. Wylie, Jr., Advanced Engineering Mathematics, McGraw-Hill Book Co., Inc., New York, 1966.

Received July 25, 1983; revised November 21, 1983

Gerald W. Baumann

IBM Information Products Division, P.O.

Box 1900, Boulder, Colorado 80302. Mr. Baumann is a senior engineer and manager of a department working on heads for flexible diskette drives. He was formerly manager of advanced fusing systems. He received a B.S. from Marquette University, Milwaukee, Wisconsin, and an M.S. from the University of Colorado, Boulder, both in mechanical engineering. In 1968, he joined IBM at the Boulder laboratory, where he worked on tape drives, copiers, collators, and currently on diskette drives. He has received a Third Level IBM Invention Achievement Award and an IBM Outstanding Innovation Award for his work in flash fusing. Mr. Baumann is a member of the American Academy of Mechanics and Sigma Xi.